Visual Motion Observer-based Pose Control via Obstacle Avoidance Navigation Function for Eye-in-Hand Systems

Yusei Tsuruo
Graduate Program in Mechanical Engineering
Kanazawa Institute of Technology
Ishikawa 921-8501, Japan
Email: integrity@venus.kanazawa-it.ac.jp

Toshiyuki Murao
Master Program of Innovation for Design and Engineering
Advanced Institute of Industrial Technology
Tokyo 140-0011, Japan
Email: murao-toshiyuki@aiit.ac.jp

Hiroyuki Kawai
Department of Robotics
Kanazawa Institute of Technology
Ishikawa 921-8501, Japan
Email: hiroyuki@neptune.kanazawa-it.ac.jp

Masayuki Fujita
Department of Mechanical and Control Engineering
Tokyo Institute of Technology
Tokyo 152-8550, Japan
Email: fujita@ctrl.titech.ac.jp

***Abstract*—This paper investigates passivity-based pose control via an obstacle avoidance navigation function for three-dimensional (3-D) eye-in-hand visual feedback systems. Firstly, visual motion observer-based pose control for 3-D eye-in-hand visual feedback systems is presented. Next, a path planner to be appropriate for the visual motion error system is designed through an obstacle avoidance navigation function to keep collision-free during servoing. Finally, the effectiveness of the proposed method is verified through computer simulations.**

I. Introduction

Visual feedback control is now a very flexible and useful method in robot control [1]. Recently, Allibert *et al.* [2] reported comparison results between two image prediction models for an image-based visual servoing scheme based on nonlinear model predictive control. Becerra *et al.* [3] presented a robust sliding mode control law that exploits epipolar geometries among three views. Zhang *et al.* [4] proposed a new 2-1/2-D visual servoing method for nonholonomic mobile robots based on a novel motion-estimation technique, which does not need homography/fundamental matrix estimation or decomposition. The authors have been proposed passivity-based visual feedback control for three-dimensional (3-D) target tracking in a series of papers [5]–[7].

Obstacle avoidance coupled with accurate path following control which is to move a vehicle towards a target location free of collisions with the obstacles has attracted much attention of a great amount of robotics researchers [8]. Huang *et al.* [9] proposed a local navigation method with a single camera for obstacle avoidance using headings to obstacles and their angular widths. Cherubini and Chaumette [10] presented appearance-based visual navigation with obstacle avoidance for real outdoor environments. This appearance-based visual navigation, which is one of the few methods for obstacle avoidance through the camera model, avoids new obstacles by using a range scanner. Although good vision-based navigation approaches for the obstacle avoidance problems are presented in [9] and [10], they are restricted to a ground vehicle.

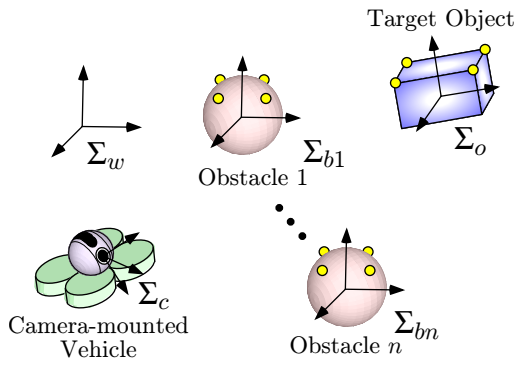

Fig. 1. Eye-in-hand visual feedback system with obstacles.

On the other hand, in robot control, one of the representative works for obstacle avoidance problems is a method using a navigation function that is globally convergent potential function proposed by Rimon and Koditschek [11]. The feature of this efficient approach is that automatically merge path finding and trajectory generation in a closed-loop fashion. Some navigation function approaches for visual feedback systems are reported in [12]–[14]. Cowan *et al.* [12] proposed a visual feedback controller to bring a robot to rest at a desired configuration for an important problem that are all feature points remain within a camera field of view by using navigation functions. Chen *et al.* [13] and the authors [14] developed an off-line path planner based on an image space navigation function with an adaptive 2 1/2-D visual servoing controller and a stabilizing receding horizon one, respectively. However, all these approaches [12]–[14] take advantage of navigation functions to solve the camera field of view problems but not to deal with the obstacle avoidance problems.

In this paper, passivity-based pose control via a navigation function for obstacle avoidance is applied to 3-D visual feedback systems with an eye-in-hand configuration as shown in

Fig. 1. Firstly, passivity-based pose control for an eye-in-hand visual motion error system is proposed. Next, a path planner to be appropriate for the visual motion error system is designed through an obstacle avoidance navigation function in order to move the camera towards a desired pose and away from obstacles without additional sensors such as a range scanner. Convergence analysis of the proposed path planner is provided. Finally, we present simulation results that demonstrate the effectiveness of the proposed control scheme.

II. Visual Motion Observer-based Pose Control

This section mainly reviews our previous work [5] via passivity-based visual feedback control with an eye-in-hand configuration.

A. Vision Camera Model

Visual feedback systems with an eye-in-hand configuration use three and n coordinate frames which consist of a world frame Σ_w, a camera frame Σ_c, a target object frame Σ_o and n obstacle frames $\Sigma_{b_1}, \cdots, \Sigma_{b_n}$ as depicted in Fig. 1. Let $p_{co} \in \mathcal{R}^3$ and $e^{\hat{\xi}\theta_{co}} \in SO(3)$ be a position vector and a rotation matrix from the camera frame Σ_c to the object frame Σ_o. Then, a relative pose from Σ_c to Σ_o can be represented by $g_{co} = (p_{co}, e^{\hat{\xi}\theta_{co}}) \in SE(3)$.

The objective of position-based visual feedback control is, in general, to bring the actual relative pose g_{co} to a reference one g_{cd}. Firstly, we consider the relative pose g_{co} in order to achieve the control objective. The relative pose from Σ_c to Σ_o can be led by using the composition rule for rigid body transformations as follows:

$$g_{co} = g_{wc}^{-1} g_{wo}. \tag{1}$$

The relative pose involves the velocity of each rigid body. To this aid, let us consider the velocity of a rigid body as described in [15]. We define the body velocity of the camera relative to the world frame Σ_w as $V_{wc}^b = [(v_{wc}^b)^T \ (\omega_{wc}^b)^T]^T$, where v_{wc}^b and ω_{wc}^b represent the velocity of the origin and the angular velocity from Σ_w to Σ_c, respectively [15].

Differentiating Eq. (1) with respect to time, the body velocity of the relative pose g_{co} can be written as follows (See [5]):

$$V_{co}^b = -\mathrm{Ad}_{(g_{co}^{-1})} V_{wc}^b + V_{wo}^b, \tag{2}$$

where V_{wo}^b is the body velocity of the target object relative to Σ_w and $\mathrm{Ad}_{(g_{co})}$ is the adjoint transformation associated with g_{co} [15].

The relative pose $g_{co} = (p_{co}, e^{\hat{\xi}\theta_{co}})$ cannot be immediately obtained in the visual feedback system, because the target object velocity V_{wo}^b is unknown and furthermore cannot be measured directly. To control the relative pose using visual information provided by computer vision system, we use the pinhole camera model with a perspective projection. Here, we consider $m(\geq 4)$ feature points on the rigid target object in this paper. Let λ be a focal length, $p_{oi} \in \mathcal{R}^3$ and $p_{ci} \in \mathcal{R}^3$ be the position vectors of the target object's i-th feature point relative to Σ_o and Σ_c, respectively. Using a transformation of the coordinates, we have $p_{ci} = g_{co} p_{oi}$, where p_{ci} and p_{oi} should be regarded, with a slight abuse of notation, as $[p_{ci}^T \ 1]^T$ and $[p_{oi}^T \ 1]^T$ via the well-known homogeneous coordinate representation in robotics, respectively (see, e.g., [15]).

The perspective projection of the i-th feature point onto the image plane gives us the image plane coordinate $f_i := [f_{xi} \ f_{yi}]^T \in \mathcal{R}^2$ as

$$f_i = \frac{\lambda}{z_{ci}} \begin{bmatrix} x_{ci} \\ y_{ci} \end{bmatrix}, \tag{3}$$

where $p_{ci} = [x_{ci} \ y_{ci} \ z_{ci}]^T$. It is straightforward to extend this model to m image points by simply stacking the vectors of the image plane coordinate, i.e., $f(g_{co}) := [f_1^T \ \cdots \ f_m^T]^T \in \mathcal{R}^{2m}$ and $p_c := [p_{c1}^T \ \cdots \ p_{cm}^T]^T \in \mathcal{R}^{3m}$. Hereafter, f_{ab} means $f(g_{ab})$ for simplicity. We assume that multiple point features on a known object are given and observed. Under this assumption, the image feature vector f_{co} depends only on the relative pose g_{co}.

B. Estimation Error System

The visual feedback control task requires information of the relative pose g_{co}. Since the measurable information is only the image feature f_{co} in the visual feedback system, we consider a nonlinear observer (we call a visual motion observer) in order to estimate the relative pose g_{co} from the image feature f_{co}.

Firstly, using Eq. (2), we choose estimates $\bar{g}_{co}$ and $\bar{V}_{co}^b$ of the relative pose and velocity, respectively as

$$\bar{V}_{co}^b = -\mathrm{Ad}_{(\bar{g}_{co}^{-1})} V_{wc}^b + u_e. \tag{4}$$

The new input u_e is to be determined in order to drive the estimated values $\bar{g}_{co}$ and $\bar{V}_{co}^b$ to their actual values.

In order to establish the estimation error system, we define the estimation error between the estimated value $\bar{g}_{co}$ and the actual relative pose g_{co} as

$$g_{ee} = \bar{g}_{co}^{-1} g_{co}. \tag{5}$$

We next define the error vector of the rotation matrix $e^{\hat{\xi}\theta_{ei}}$ as $r_{ei} := \mathrm{sk}(e^{\hat{\xi}\theta_{ei}})^\vee$ where $\mathrm{sk}(e^{\hat{\xi}\theta_{ei}})$ denotes $\frac{1}{2}(e^{\hat{\xi}\theta_{ei}} - e^{-\hat{\xi}\theta_{ei}})$. Using this notation, the vector of the estimation error is given by $e_e := [p_{ee}^T \ r_{ee}^T]^T$.

Suppose the attitude estimation error θ_{ee} is small enough that we can let $e^{\hat{\xi}\theta_{ee}} \simeq I + \mathrm{sk}(e^{\hat{\xi}\theta_{ee}})$. Therefore, using a first-order Taylor expansion approximation, the estimation error vector e_e can be obtained from image information f_{co} and the estimated value of the relative pose $\bar{g}_{co}$ as follows:

$$e_e = J_e^\dagger(\bar{g}_{co})(f_{co} - \bar{f}_{co}), \tag{6}$$

where $\bar{f}_{co}$ is the estimated value of image feature and $J_e(\bar{g}_{co})$ is an image Jacobian-like matrix [5]. In the same way as Eq. (2), the estimation error system can be represented by

$$V_{ee}^b = -\mathrm{Ad}_{(g_{ee}^{-1})} u_e + V_{wo}^b. \tag{7}$$

C. Pose Control Error System

Let us consider the dual of the estimation error system, which we call the pose control error system in order to achieve the control objective. Firstly, we define the pose control error as follows:

$$g_{ec} = g_{cd}^{-1} g_{co}, \tag{8}$$

which represents the error between the relative pose g_{co} and the reference one g_{cd}. It should be remarked that g_{co} can be calculated by using the estimated relative pose $\bar{g}_{co}$ and the estimation error vector $e_e = [p_{ee}^T \ r_{ee}^T]^T$ equivalently as follows:

$$g_{co} = \bar{g}_{co} g_{ee} \tag{9}$$

$$\xi\theta_{ee} = \frac{\sin^{-1}\|r_{ee}\|}{\|r_{ee}\|} r_{ee}, \tag{10}$$

although g_{co} cannot be measured directly. Similar to the estimation error vector, the vector of the pose control error is defined as $e_c := [p_{ec}^T \ r_{ec}^T]^T$.

Differentiating Eq. (8) with respect to time, the pose control error system can be represented as

$$V_{ec}^b = -\mathrm{Ad}_{(g_{ec}^{-1})}\left(\mathrm{Ad}_{(g_{cd}^{-1})} V_{wc}^b + V_{cd}^b\right) + V_{wo}^b, \tag{11}$$

where V_{cd}^b is the body velocity of the reference of the relative pose g_{cd}.

D. Visual Motion Observer-based Pose Control

Combining the estimation error system (7) and the pose control one (11), we construct the visual motion observer-based pose control error system (we call the visual motion error system) as follows:

$$\begin{bmatrix} V_{ec}^b \\ V_{ee}^b \end{bmatrix} = \begin{bmatrix} -\mathrm{Ad}_{(g_{ec}^{-1})} & 0 \\ 0 & -\mathrm{Ad}_{(g_{ee}^{-1})} \end{bmatrix} u + \begin{bmatrix} I \\ I \end{bmatrix} V_{wo}^b, \tag{12}$$

where

$$u := [u_c^T \ u_e^T]^T, \ u_c := \mathrm{Ad}_{(g_{cd}^{-1})} V_{wc}^b + V_{cd}^b. \tag{13}$$

Let us define the error vector of the visual motion error system as $x := [e_c^T \ e_e^T]^T$, which consists of the pose control error vector e_c and the estimation error vector e_e. It should be noted that if the vectors of the pose control error and the estimation one are equal to zero, then the actual relative pose g_{co} tends to the reference one g_{cd} when $x \to 0$.

It can be proved that the visual motion error system (12) is passive from the input u to the output $-x$ by using the following positive definite function:

$$V = E(g_{ec}) + E(g_{ee}), \tag{14}$$

where $E(g_{ei}) := \frac{1}{2}\|p_{ei}\|^2 + \phi(e^{\hat{\xi}\theta_{ei}})$ and $\phi(e^{\hat{\xi}\theta_{ei}}) := \frac{1}{2}\mathrm{tr}(I - e^{\hat{\xi}\theta_{ei}})$ is an error function of the rotation matrix.

Based on the passivity property of the visual motion error system, we consider the following control law.

$$u = -K(-x), \ K := \mathrm{diag}\{K_c, K_e\}, \tag{15}$$

where $K_c := \mathrm{diag}\{k_{c1}, \cdots, k_{c6}\}$ and $K_e := \mathrm{diag}\{k_{e1}, \cdots, k_{e6}\}$ are the positive gain matrices of x, y and z axes of the translation and the rotation for the pose control error and the estimation one, respectively.

Theorem 1 ([5]): If $V_{wo}^b = 0$, then the equilibrium point $x = 0$ for the closed-loop system (12) and (15) is asymptotic stable.

Theorem 1 shows Lyapunov stability for the closed-loop system. If the camera velocity V_{wc}^b is decided directly, the control objective is achieved by using the proposed control law (15).

III. Obstacle Avoidance Navigation Function-based Path Planning for Eye-in-Hand Systems

Vision-based navigation with obstacle avoidance should offer great perspectives in many applications, such as surveillance, patrolling, search and rescue or high risk missions. In this section, as a first step for a vision-based navigation, we design a path planer through an obstacle avoidance navigation function for 3-D eye-in-hand visual feedback systems. The control objective in this paper is stated as follows:

Control Objective: The camera follows the target object, i.e., the relative pose $g_{co}(t)$ is coincided with the time-varying desired one $g_{cd}(t)$ which is generated to avoid unexpected obstacles, and which converges the final desired one g_{cd_f}.

From the proposed visual feedback control law, the input to the camera is designed as follows:

$$V_{wc}^b = \mathrm{Ad}_{(g_{cd})}\left(u_c - V_{cd}^b\right). \tag{16}$$

Hence, the camera input is needed the body velocity $V_{cd}^b = [(v_{cd}^b)^T \ (\omega_{cd}^b)^T]^T$ of the reference of the relative pose g_{cd}[1].

A. Rotation Error for Path Planning

In rotation control, we consider only convergence to the final desired rotation. We define the rotation error between the time-varying relative desired rotation $e^{\hat{\xi}\theta_{cd}}$ and the final one $e^{\hat{\xi}\theta_{cd_f}}$ as follows:

$$e^{\hat{\xi}\theta_{ed}} = e^{-\hat{\xi}\theta_{cd_f}} e^{\hat{\xi}\theta_{cd}}. \tag{17}$$

The vector form is defined as $r_{ed} := \mathrm{sk}(e^{\hat{\xi}\theta_{ed}})$. Differentiating Eq. (17) with respect to time, the rotation error system for path planning can be written as

$$\omega_{ed}^b = \omega_{cd}^b. \tag{18}$$

B. Visual Motion Observer for Path Planning

Obstacle avoidance navigation function-based path planning needs the relative position of the obstacles from the camera frame p_{cb_i}. In this section, we design the visual motion observer in order to estimate the relative position p_{cb_i} using the image feature $f_{cb_i} := f(g_{cb_i})$. Now, we assume that the multiple points on the obstacles can be observed and the

[1]The relative pose g_{cd} can be obtained solving $\dot{g}_{cd} = g_{cd}\hat{V}_{cd}^b$.

position of them $p_{b_i i}$ is known. The body velocity of the relative pose g_{cb_i} can be written as follows:

$$V^b_{cb_i} = -\mathrm{Ad}_{(g^{-1}_{cb_i})} V^b_{wc} + V^b_{wb_i}, \tag{19}$$

where $V^b_{wb_i}$ is the i-th obstacle body velocity. Using the body velocity $V^b_{cb_i}$ (19), we establish a following estimate model for the obstacles:

$$\bar{V}^b_{cb_i} = -\mathrm{Ad}_{(\bar{g}^{-1}_{cb_i})} V^b_{wc} + u_{b_i}, \tag{20}$$

where $\bar{g}_{cb_i}$ and $\bar{V}^b_{cb_i}$ are the estimated values of g_{cb_i} and $V^b_{cb_i}$, respectively. We define the estimation error g_{eb_i} between the actual relative pose g_{cb_i} and the estimated one $\bar{g}_{cb_i}$ as follows:

$$g_{eb_i} = \bar{g}^{-1}_{cb_i} g_{cb_i}. \tag{21}$$

The vector of the estimation error $e_{b_i} = [p^T_{eb_i}\ r^T_{eb_i}]^T$ can be obtained by exploiting the image feature f_{cb_i} and the estimate values $\bar{g}_{cb_i}$ and $\bar{f}_{cb_i}$ as

$$e_{b_i} = J^{\dagger}_e(\bar{g}_{cb_i})(f_{cb_i} - \bar{f}_{cb_i}). \tag{22}$$

Hence, the relative position p_{cb_i} can be calculated as follows:

$$p_{cb_i} = e^{\hat{\bar{\xi}}\bar{\theta}_{cb_i}} p_{eb_i} + \bar{p}_{cb_i} \tag{23}$$

through $g_{cb_i} = \bar{g}_{cb_i} g_{eb_i}$. The estimation error system for the obstacles can be obtained as

$$V^b_{eb_i} = -\mathrm{Ad}_{(g^{-1}_{eb_i})} u_{b_i} + V^b_{wb_i}. \tag{24}$$

C. Obstacle Avoidance Navigation Function

In this subsection, we develop the obstacle avoidance navigation function $\varphi(p_{cd})$ [11], [16]. In this paper, we assume that the workspace and the obstacles are spherical. This assumption does not constrain the generality of this work since it has been proven that navigation properties are invariant under diffeomorphisms in [16].

Firstly, we define a space D where the camera can move avoiding obstacles as follows:

$$D = F - \bigcup_{i=1}^{M} B_i, \tag{25}$$

where $F := \{p_{cd} : \|p_{cd}\|^2 \leq \rho_0^2\}$ is the camera movable space which represents a Euclidean 3-dimensional disk with the radius $\rho_0 > 0$, and $B_i := \{p_{cd} : \|p_{cb_i}(p_{cd})\|^2 < \rho_i^2\},\ i = 1 \dots M$ denotes a M-th obstacle space in F with the radius $\rho_i > 0$. We impose the additional constraint that all obstacles closures are contained in the interior of the workspace; i.e. $\|p_{cb_i}\| + \rho_i < \rho_0,\ 1 \leq i \leq M$, and that none of them intersect; i.e. $\|p_{cb_i} - p_{cb_j}\| > \rho_i + \rho_j,\ 1 \leq i, j \leq M$. If $p_{cd} \in D$, the camera keeps collision-free.

The navigation functions used in this paper are defined as follows:

Definition 1 ([11],[16]): A smooth Morse function $\varphi(p_{cd}) : D \to [0, 1]$ is a navigation function if it is

1) a unique minimum exists at p_{cd_f};
2) uniformly maximal on the boundary of D.

A smooth vector field on any sphere world with a unique attractor, must have at least as many saddles as obstacles. The property of a Morse function whose Hessian at all critical points is non-degenerate establishes that the initial conditions that bring the system to saddle points are sets of measure zero. In view of this property, all initial conditions away from sets of measure zero are brought to the unique minimum [16].

In order to design the obstacle avoidance navigation function, we utilize the following function which represents the error between the desired relative position p_{cd} and the final one p_{cd_f}:

$$s(p_{cd}) = \|p_{cd} - p_{cd_f}\|^{2\kappa}, \tag{26}$$

where $\kappa > 0 \in \mathcal{R}$ is an additional parameter to change the potential field. Next, let define the obstacle function which includes the function η_0 for keeping in the space F as

$$\eta(p_{cd}) = \prod_{i=0}^{M} \eta_i(p_{cd}) \tag{27}$$

$$\eta_i(p_{cd}) = \begin{cases} \rho_0^2 - \|p_{cd}\|^2 & \text{for } i = 0 \\ \|p_{cb_i}\|^2 - \rho_i^2. & \text{for } i = 1 \cdots M \end{cases}$$

Then, the model space navigation function $\tilde{\varphi}(x) \in \mathcal{R}^{2m} \to [0, 1]$ and a κ-th root function are defined as

$$\tilde{\varphi}(x) = \frac{x}{\mu + x} \tag{28}$$

and

$$\rho(x) = x^{\frac{1}{\kappa}}, \tag{29}$$

respectively, where $\mu > 0 \in \mathcal{R}$ is a parameter. The function (29) is important in order to change p_{cd_f} to a non-degenerate critical point. From Eqs. (26)–(29), the obstacle avoidance navigation function denoted by $\varphi(p_{cd}) \in D \to \mathcal{R}$, can be developed as follows:

$$\varphi(p_{cd}) = \rho \circ \tilde{\varphi} \circ \frac{s}{\eta}(p_{cd}) = \left(\frac{s(p_{cd})}{\mu\eta(p_{cd}) + s(p_{cd})} \right)^{\frac{1}{\kappa}} \tag{30}$$

where $\circ$ denotes the composition operator. Using a similar way in [16], it can be verified that the function (30) is the navigation function if the parameter κ is selected adequately.

D. Path Planning of Desired Body Velocity

We design the desired body velocity V^b_{cd} and the input for the estimation u_{b_i} as follows:

$$V^b_{cd} = \begin{bmatrix} -e^{-\hat{\xi}\theta_{cd}} K_{dp} \nabla\varphi(p_{cd}) \\ -K_{dr} e^{-\hat{\xi}\theta_{ed}} r_{ed} \end{bmatrix} \tag{31}$$

$$u_{b_i} = K_b e_{b_i}, \tag{32}$$

where $K_{dp} := \mathrm{diag}\{k_{dp1}, k_{dp2}, k_{dp3}\}$, $K_{dr} := \mathrm{diag}\{k_{dr1}, k_{dr2}, k_{dr3}\}$ and $K_b := \mathrm{diag}\{k_{b1}, \cdots, k_{b6}\}$ are the positive gain matrices for the translation and the rotation of the desired body velocity and for the estimation input, respectively. $\nabla\varphi(p_{cd}) := \left(\frac{\partial\varphi(p_{cd})}{\partial p_{cd}}\right)^T$ which denotes

the gradient vector of $\varphi(p_{cd})$ can be calculated as Eq. (33) at the bottom of this page.

We state the main result of this paper concerning the convergence of the path planner.

Theorem 2: Suppose that $V_{wo}^b = 0$ and $V_{wb_i}^b = 0$, and the initial desired relative position $p_{cd}(0)$ satisfies $p_{cd}(0) \in D$. Then, the desired relative position $p_{cd}(t)$ ensures that $p_{cd}(t) \in D$ and $g_{cd}(t)$ has the asymptotically stable equilibrium point g_{cd_f}.

Proof: Consider the following positive definite function:

$$V_n = \varphi(p_{cd}) + \phi(e^{\hat{\xi}\theta_{ed}}) + \sum_{i=1}^{M} E(g_{eb_i}). \tag{34}$$

Evaluating the time derivative of V_n along the trajectories of Eqs. (18), (24), (31), (32) gives us

$$\begin{aligned}
\dot{V}_n &= (\nabla\varphi)^T \dot{p}_{cd} + r_{ed}^T e^{\hat{\xi}\theta_{ed}} \omega_{ed}^b + \sum_{i=1}^{M} e_{b_i}^T \mathrm{Ad}_{(e^{\hat{\xi}\theta_{eb_i}})} V_{eb_i}^b \\
&= (\nabla\varphi)^T e^{\hat{\xi}\theta_{cd}} v_{cd}^b + r_{ed}^T e^{\hat{\xi}\theta_{ed}} \omega_{cd}^b \\
&\quad + \sum_{i=1}^{M} e_{b_i}^T \mathrm{Ad}_{(e^{\hat{\xi}\theta_{eb_i}})} (-\mathrm{Ad}_{(g_{eb_i})}^{-1} u_{b_i}) \\
&= -(\nabla\varphi)^T e^{\hat{\xi}\theta_{cd}} e^{-\hat{\xi}\theta_{cd}} K_{dp} \nabla\varphi - r_{ed}^T e^{\hat{\xi}\theta_{ed}} K_{dr} e^{-\hat{\xi}\theta_{ed}} r_{ed} \\
&\quad + \sum_{i=1}^{M} \left(-e_{b_i}^T K_b e_{b_i} \right) \\
&= -(\nabla\varphi)^T K_{dp} \nabla\varphi - (e^{-\hat{\xi}\theta_{ed}} r_{ed})^T K_{dr} e^{-\hat{\xi}\theta_{ed}} r_{ed} \\
&\quad - \sum_{i=1}^{M} e_{b_i}^T K_b e_{b_i}.
\end{aligned} \tag{35}$$

It is clear from Eq. (35) that V_n is a non-increasing function in the sense that

$$V_n \leq V_n(0). \tag{36}$$

From Eqs. (34) and (36), the condition $p_{cd}(t) \in D$, $\forall t > 0$ is satisfied for any initial condition $p_{cd}(0) \in D$. Since the estimation error vector $e_{b_i} \to 0$, the position p_{cb_i} which is utilized in the obstacle functions converges actual value. Thanks to the property of navigation functions [16], it can be shown $p_{cd}(t) \to p_{cd_f}$ through $\nabla\varphi(p_{cd}) \to 0$. On the other hand, the rotation $e^{\hat{\xi}\theta_{cd}}(t) \to e^{\hat{\xi}\theta_{ed_f}}$ can be verified because of $e^{-\hat{\xi}\theta_{ed}} r_{ed} \to 0$. Therefore, it can be concluded that $g_{cd}(t) \to g_{cd_f}$. ■

Theorem 2 guarantees the convergence of the time-varying desired pose $g_{cd}(t)$ to the final one g_{cd_f}. The path planner can be designed to keep collision-free based on the obstacle avoidance navigation function. The block diagram of the visual motion observer-based eye-in-hand pose control with the obstacle avoidance navigation function-based path planner is shown in Fig. 2.

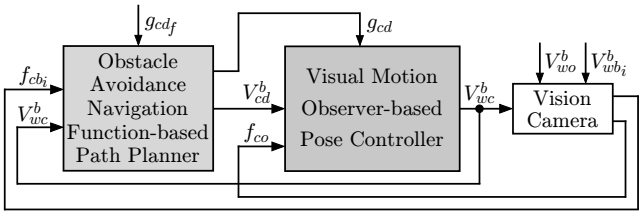

Fig. 2. Block diagram of visual motion observer-based eye-in-hand pose control with obstacle avoidance navigation function-based path planner.

Our proposed approach, which deals with the estimation problem from the visual features explicitly, can be applied to 3-D eye-in-hand visual feedback systems without restriction to the ground vehicle. Thus, the proposed method which is connected the visual motion observer-based pose control and the obstacle avoidance navigation function-based path planner without additional sensors allows us to extend technological application area. The main contribution of this paper is to provide that the path planner which can achieve obstacle avoidance during the servoing is designed for the eye-in-hand visual feedback control.

In our passivity-based visual feedback control approach, the image Jacobian-like matrix $J(\cdot)$ of the pinhole camera model is exactly the same form as that of the panoramic camera model [17]. Therefore, the proposed approach can be applied to 3-D eye-in-hand visual feedback systems with a panoramic camera using the image Jacobian-like matrix $J(\cdot)$ in [17].

IV. Verification

In this section, we present simulation results for the visual feedback control with the path planner via the obstacle avoidance navigation function, compared with the constant desired relative pose proposed in [5]. The control objective is that the camera tracks the static target object to avoid two obstacles. In other words, it is bring the actual relative pose $g_{co}(t)$ to a given reference one g_{cd_f} using a time-varying reference one $g_{cd}(t)$, and it can be achieved to make both the estimation and the pose control errors zero.

The simulation is carried out with the initial condition $p_{co} = [-1.25\ 4.994\ 0.5]^T$ m, $\xi\theta_{co} = [0\ 0\ -\pi/12]^T$ rad. The final desired relative pose is $p_{cd_f} = [0\ 1.5\ 0]^T$ m, $\xi\theta_{cd_f} = [0\ 0\ 0]^T$ rad. The other conditions are set as $p_{cb_1} = [-0.224\ 1.095\ 0]^T$ m, $\xi\theta_{cb_1} = [0\ 0\ -\pi/12]^T$ rad, $\rho_1 = 0.5$ m, $p_{cb_2} = [-1.414\ 2.45\ 0.75]^T$ m, $\xi\theta_{cb_2} = [0\ 0\ -\pi/12]^T$ rad, $\rho_2 = 0.5$ m.

The simulation results are presented in Figs. 3 and 4. Fig. 3 shows the actual pose control error e_r, which is the error vector between the current relative pose $g_{co}(t)$ and the final desired one g_{cd_f}. The asymptotic stability can be confirmed by steady state performance in Fig. 3.

$$\nabla\varphi(p_{cd}) = \frac{2\mu}{\kappa(\mu\eta + s)^{\frac{1+\kappa}{\kappa}}} \left(\kappa\eta(p_{cd} - p_{cd_f}) + \|p_{cd} - p_{cd_f}\|^2 \left(\prod_{i=1}^{M} \eta_i p_{cd} - \sum_{j=1}^{M} \prod_{i=0, i\neq j}^{M} \eta_i p_{cb_j} \right) \right) \tag{33}$$

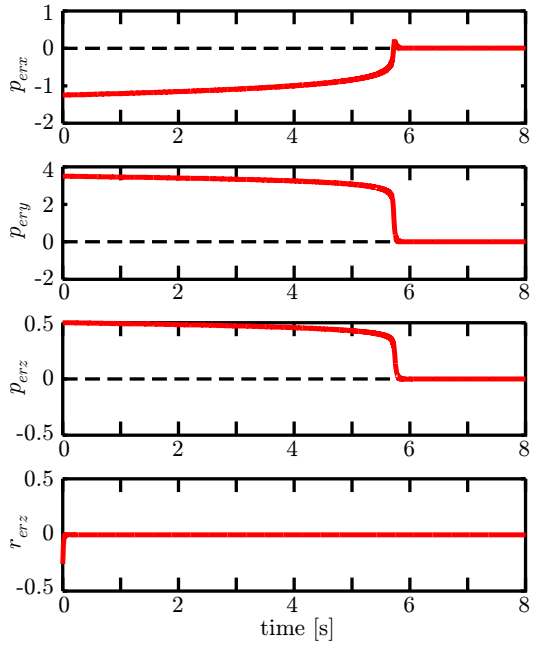

Fig. 3. Pose control error $e_r(p_{erx}, p_{ery}, p_{erz}, r_{erz})$.

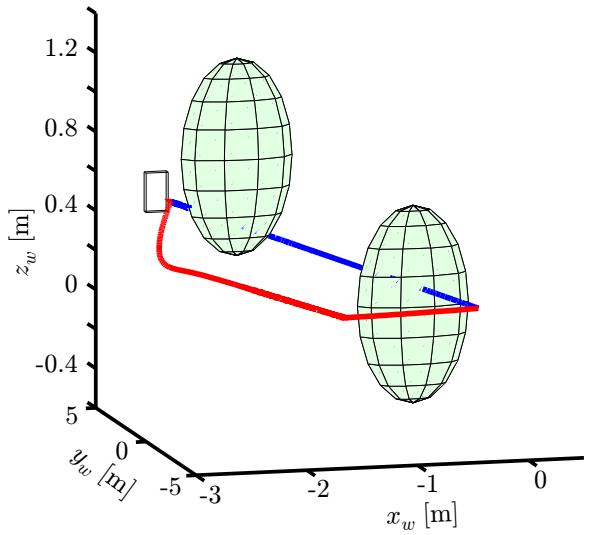

Fig. 4. Trajectory of position p_{wc} with two obstacles: Solid (Red); applying proposed method: Dashed (Blue); applying previous one[5].

Fig. 4 presents the trajectory of the position of the camera p_{wc}. In Fig. 4, the spheres and the rectangle show the static obstacles and target object, respectively. The solid (red) lines denote the trajectory applying the proposed passivity-based pose control with the path planner, and the dashed (blue) lines denote those with the constant desired value. The trajectory should be designed that the camera moves toward the rectangle avoiding the spheres. From Fig. 4, it is concluded that the proposed method can make the camera avoid all obstacles. Although the convergence to the desired values is also achieved in the case of the previous method [5] in the simulation, it corresponds to fail in the actual experiment since the camera hits the obstacles.

V. Conclusions

This paper proposes passivity-based 3-D eye-in-hand visual feedback control via an obstacle avoidance navigation function. The main contribution of this paper is to show that the path planner which can avoid obstacles during servoing is designed for 3-D eye-in-hand visual feedback systems. Simulation results are presented to verify the control performance of the proposed control scheme with obstacle avoidance. Although only simulation results are shown in this submitted version, experimental movies using a Parrot AR.Drone which is a wifi quadrotor aerial vehicle with two cameras are available at `http://wwwr.kanazawa-it.ac.jp/kawai/research/ARDrone/ARDronemovies.html`.

References

[1] F. Chaumette and S. A. Hutchinson, "Visual Servoing and Visual Tracking," In:B. Siciliano and O. Khatib (Eds), *Springer Handbook of Robotics*, Springer–Verlag, pp. 563–583, 2008.

[2] G. Allibert, E. Courtial and F. Chaumette, "Predictive Control for Constrained Image-based Visual Servoing," *IEEE Trans. Robotics*, Vol. 26, No. 5, pp. 933–939, 2010.

[3] H. M. Becerra, G. López-Nicolás and C. Sagüés, "A Sliding-mode-control Law for Mobile Robots based on Epipolar Visual Servoing from Three Views," *IEEE Trans. Robotics*, Vol. 27, No. 1, pp. 175–183, 2011.

[4] X. Zhang, Y. Fang and Xi Liu, "Motion-estimation-based Visual Servoing of Nonholonomic Mobile Robots," *IEEE Trans. Robotics*, Vol. 27, No. 6, pp. 1167–1175, 2011.

[5] M. Fujita, H. Kawai and M. W. Spong, "Passivity-based Dynamic Visual Feedback Control for Three Dimensional Target Tracking: Stability and L_2-gain Performance Analysis," *IEEE Trans. Control Systems Technology*, Vol. 15, No. 1, pp. 40–52, 2007.

[6] T. Murao, H. Kawai and M. Fujita, "Passivity-based Control of Dynamic Visual Feedback Systems with Movable Camera Configuration," *Electronics and Communications in Japan*, Vol. 92, No. 6, pp. 1–11, 2009.

[7] T. Murao, H. Kawai and M. Fujita, "Stabilizing Predictive Visual Feedback Control for Fixed Camera Systems," *Electronics and Communications in Japan*, Vol. 94, No. 8, pp. 1–11, 2011.

[8] J. Minguez, F. Lamiraux and J.-P. Laumond, "Motion Planning and Obstacle Avoidance," In:B. Siciliano and O. Khatib (Eds), *Springer Handbook of Robotics*, Springer–Verlag, pp. 827–852, 2008.

[9] W. H. Huang, B. R. Fajen, J. R. Fink and W. H. Warren, "Visual Navigation and Obstacle Avoidance using a Steering Potential Function," *Robotics and Autonomous Systems*, Vol. 54, No. 4, pp. 288–299, 2006.

[10] A. Cherubini and F. Chaumette, "Visual Navigation with Obstacle Avoidance," *Proc. 2011 IEEE/RSJ International Conference on Intelligent Robots and Systems*, pp. 1593–1598, 2011.

[11] E. Rimon and D. E. Koditschek, "Exact Robot Navigation using Artificial Potential Functions," *IEEE Trans. Robotics and Automation*, Vol. 8, No. 5, pp. 501–518, 1992.

[12] N. J. Cowan, J. D. Weingarten and D. E. Koditschek, "Visual Servoing via Navigation Functions," *IEEE Trans. Robotics and Automation*, Vol. 18, No. 4, pp. 521–533, 2002.

[13] J. Chen, D. M. Dawson, W. E. Dixon and V. K. Chitrakaran, "Navigation Function-based Visual Servo Control," *Automatica*, Vol. 43, No. 7, pp. 1165–1177, 2007.

[14] T. Murao H. Kawai and M. Fujita, "Visual Motion Observer-based Stabilizing Receding Horizon Control via Image Space Navigation Function," *Proc. of the 2010 IEEE Multi-conference on Systems and Control*, pp. 1648–1653, 2010.

[15] R. Murray, Z. Li and S. S. Sastry, *A Mathematical Introduction to Robotic Manipulation*, CRC Press, 1994.

[16] D. E. Koditschek and E. Rimon, "Robot Navigation Functions on Manifolds with Boundary," *Advances in Applied Mathematics*, Vol. 11, No. 4, pp. 412–442, 1990.

[17] H. Kawai, T. Murao and M. Fujita, "Passivity-based Visual Motion Observer with Panoramic Camera for Pose Control," *Journal of Intelligent and Robotic Systems*, Vol. 64, No. 3–4, pp. 561–583, 2011.